A Capacitance-based System Design for Measurement of Crude Oil Moisture

ZhixueShi, Xudong Zhao*
Department of Computer Science and Technology, College of Computer and Control Engineering,
Northeast Forestry University, Harbin, China

***Abstract*—Challenges including difficulty in cleaning and low measurement accuracy widely exist in traditional methods for measuring moisture in crude oil. In order to solve these problems, a capacitance measurement device that combines PCAP01 and STM32 has been designed. PCAP01 is employed as the processing core of the sensor, which significantly enhances the measurement accuracy of capacitance-based methods. As to STM32, it plays a critical role in data acquisition, signal processing, and data transmission. Besides, the capacitance-based device contains two symmetric half-cylindrical electrode plates that are closely attached to the outer wall of the cylindrical glass vessel, where the crude oil sample to be tested is contained. This design prevents the direct contact between the liquid sample and the electrode plates, thus eliminating issues related to cleaning difficulties. Time-frequency domain expansion is presented to realize the fit between moisture and the capacitance. Experimental results indicate that the designed system delivers a high accuracy across the entire 0-100% range.**

***Keywords*—Capacitance measurement; crude oil moisture; PCAP01; STM32; time-frequency domain**

I. Introduction

Measurement of water content in crude oil is crucial to petroleum extraction and petrochemical industry [1]-[3]. It stands as a pivotal parameter in oilfield production and petroleum trade, exerting significant influence over the extraction, dehydration, storage, sales, and refining phases of crude oil. Inaccurate monitoring of crude oil moisture can affect many aspects, such as determination of water influx in oil wells, identification of oil-bearing formations, estimation of crude oil production, prediction of the lifespan of oil wells, and the operations of downstream enterprises. Several techniques can be employed to assess moisture in crude oil, encompassing well-established approaches like the classical distillation method [4, 5]. Although this method has high measurement accuracy, it is quite time-consuming. Besides, it is difficult to clean the device. Sometimes, it is of trouble to preserve the chemical agent used for water removal.

One study has determined the moisture content in crude oil by estimating the density of crude oil [6]. However, this complex method is difficult to operate. As a result, non-contact measurements are taken into account. It is known that electromagnetic waves can be absorbed by water in crude oil. Thus, ultrasound [7]-[9], microwave [10]-[14], near infrared ray [15], gamma ray [16], terahertz [17, 18], radio frequency [19]-[21], etc. are used to calculate the ratio of the water content in crude oil. Anyway, these methods need an independent calibration before each measurement. The corresponding devices also have poor portability. Instead of electromagnetic waves, an image processing technique has been utilized for visual measurement of water content in crude oil [22]. After electric dehydration, an image of oil-water stratification is obtained. Then, a grayscale accumulated value difference is made to obtain the coordinate values of the layered interface to calculate the ratio of water to crude oil. However, it's worth noting that the procedure of electric dehydration is time-consuming.

Correspondingly, contact measurement methods have appeared. Because of having different dielectric constants, a change of water content in crude oil may lead to a change in its capacitance value, which may convert to a variation of an oscillator's phase angle [23] or a change to the oscillation frequency of a non-contact frequency modulated oscillator's output [24]. Although the contact measurement methods have great accuracies, the indirect measurements of the capacitance value correspond to a poor range, which is limited by the oil-water ratio of the tested crude oil [25, 26].

To address the issues of electrode plate cleaning difficulty and low accuracy in the full-range measurement of the capacitive method, this paper proposes a non-contact capacitive measurement scheme for crude oil and develops a crude oil moisture content detection system. Two symmetric cylindrical electrode plates are designed as the sensing probes, which effectively prevents crude oil from corroding the electrode plates. The designed non-intrusive capacitance sensor also employs a PCAP01 chip, which can measure subtle changes in PF level, to obtain the capacitance value. Besides, a STM32 chip is selected as the data control unit. The symmetric cylindrical electrode plates, PCAP01, STM32 and their relevant circuit constitute a capacitance measurement device. In addition, time-frequency domain expansion is used in an upper machine. Together, they form a system for measurement of crude oil moisture. Experiments have been conducted to measure the water content in different crude oil samples. Corresponding results demonstrate the effectiveness of our method.

II. Design Methods

A. Sensor Probe Design

Actually, crude oil can be treated as a mixture of pure water and pure oil after removing gas. At room temperature, crude oil possesses a relative dielectric constant of 2.2; while, pure water exhibits a relative dielectric constant of 80. Therefore, different

*Corresponding Author.

relative dielectric constants corresponding to different capacitance values have different ratios of the water content in crude oil. In the measurement procedure, crude oil sample is introduced into a cylindrical glass vessel. The overall capacitance comprises the capacitances connected in series including the capacitance of the glass wall and the one of crude oil. The overall capacitance is expressed as follows,

$$C = \frac{C_g C_r}{C_g + C_r}, \quad (1)$$

Where C represents the total capacitance measured by the sensor. C_r and C_g denotes the capacitance value of the crude oil and theglass wall, respectively. Correspondingly, the dielectric constant of the glass wall, which is determined by the material properties of the glass, can be considered a constant.

A slotted cylindrical capacitor is designed to be the sensing probe for capacitance sensing, as shown in Fig. 1. Unlike traditional parallel-plate capacitors, the slotted cylindrical capacitor offers a more uniform electric field distribution, allowing for a more precise measurement of sample properties. Furthermore, due to its symmetrical design, the measurement results of the slotted cylindrical capacitor remain unaffected by the rotation direction of the tested sample, enhancing its practicality. In actual measurements, it is essential to securely attach the slotted cylindrical electrode plates to the glass vessel to eliminate any interference caused by air between the electrode plate and the vessel.

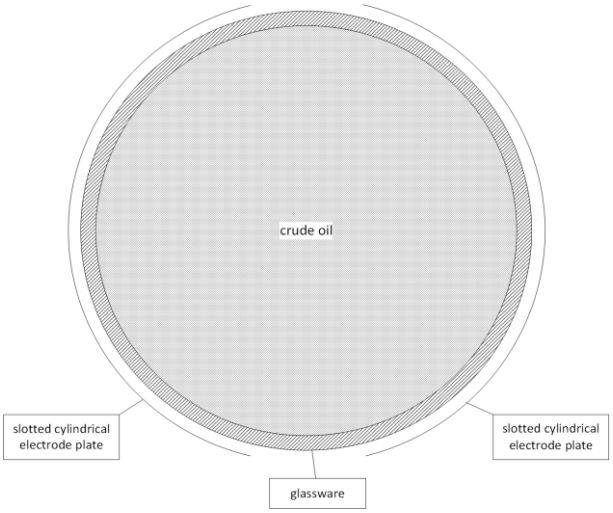

Fig. 1. The top view of the device's structure.

B. Measuring Principle

Correspondingly, the capacitance for the slotted cylindrical capacitor [27] can be expressed as follows,

$$C = \sum_{i=1}^{n} 2 * \varepsilon_0 * \varepsilon_r * A * \left[\frac{1}{d + (i-1)\Delta d}\right] + \frac{\varepsilon_0 * \varepsilon_r * A}{2R}, \quad (2)$$

where C denotes the capacitance value measured by the slotted cylindrical capacitor. ε_0 represents the absolute permittivity with ε_0 = 8.85×10-12 (F/m). ε_r represents the relative permittivity of the water-containing crude oil. A is the unit surface area of the slotted cylindrical capacitor. R denotes the radius of the slotted cylindrical plates. n is the cutting number for numerical analysis. d is the minimum gap distance. Δd is an increment distance.

The effective permittivity of the crude oil, which mainly depends on volume percentage of two phases in container, is given by [23]

$$\varepsilon_r = \alpha * \varepsilon_w + (1 - \alpha) * \varepsilon_i, \quad (3)$$

where ε_w, ε_i and ε_r represent the relative permittivity of pure water, pure oil and the crude oil sample, respectively. α denotes the ratio of the water content in the crude oil sample.

It can be seen in Eq. (2) that C and ε_r show a linear correlation. Besides, there is a linear relationship between ε_r and α, as expressed in Eq. (3). That is, the capacitance for the slotted cylindrical capacitor is in direct proportion to the ratio of the water content in crude oil.

C. System Hardware Design

To achieve precise measurement of water content in crude oil, a capacitance measurement device is designed. In addition to the presented symmetric cylindrical electrode plates which are regarded as the sensor probe, the proposed device also includes PCAP01, STM32 and their relevant circuit. The device primarily comprises the sensor probe, a sensor module, a processing module, a communication module, a power supply module, and a personal computer, as depicted in Fig. 2.

In Fig. 2, the crude oil sample is loaded into the glassware of the designed sensing probe (see Fig. 1.). The sensor module uses the PACP01-AD as the core chip to collect the capacitance values from the probe. The corresponding circuit configuration is shown in Fig. 3. The circuit, which is capable of simultaneously measuring 4 different capacitance values, adopts the drift mode for capacitance measurement with 8 interfaces PC0-PC7. As the PACP01-AD chip uses the charge-discharge time for capacitance measurement, it is necessary to connect reference capacitances to PC0 and PC1 according to the actual range. As a result, 47pf high-precision capacitors are soldered to PC0 and PC1 as the reference capacitors. The sensor module communicates with the processing module using SPI, mainly due to the faster communication speed compared to IIC. Additionally, an LED light is added to PG3 to indicate the working status of the sensor. It is worth noting that although the official manual states that when using SPI communication, the IIC_EN pin should be grounded or left floating, it has been found in practical applications that leaving it floating may occasionally lead to SPI communication failures. Therefore, it is important to ground the IIC_EN pin to ensure normal SPI communication.

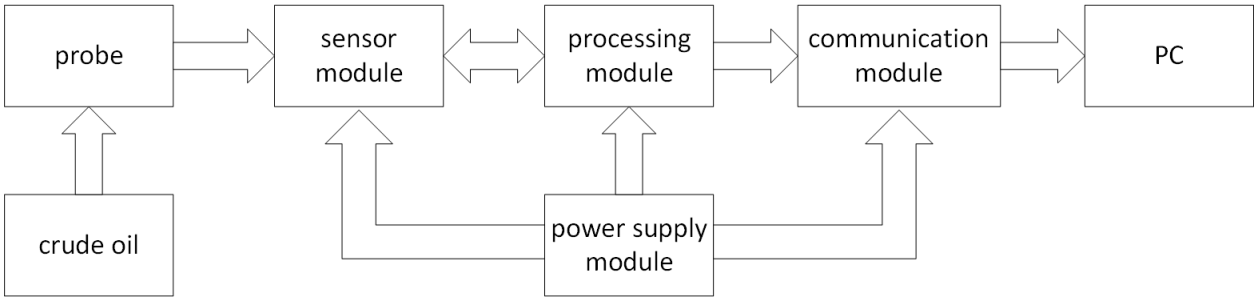

Fig. 2. System hardware diagram.

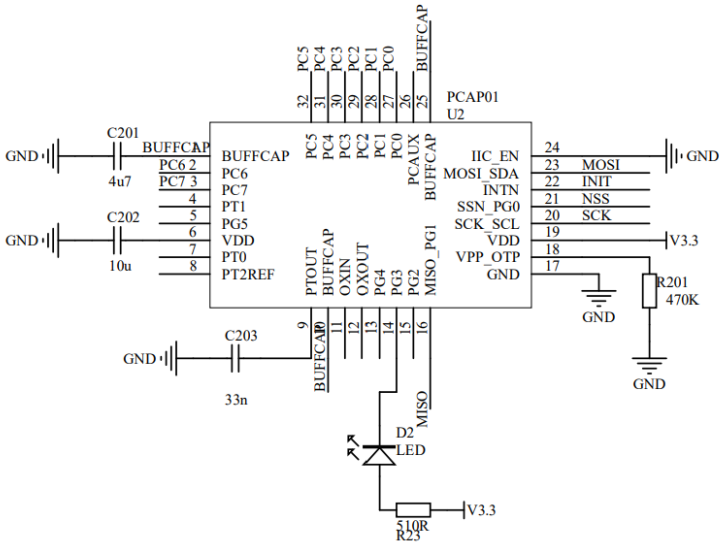

Fig. 3. PACP01 circuit diagram.

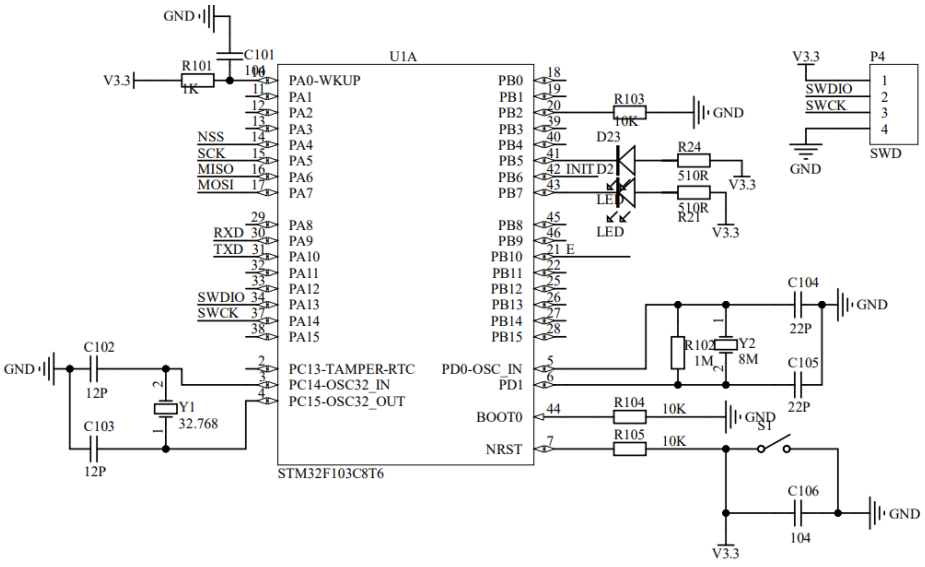

Fig. 4. STM32F103C8T6 circuit diagram.

As illustrated in Fig. 4, the circuit configuration which is associated with the processing module is based on the STM32F103C8T6 minimum system, with additional LED lights on PB5 and PB7 pins to indicate the system's operation status. The PA4, PA5, PA6, and PA7 pins are also brought out for communication with the sensor module, while PA9 and PA10 pins are used for RXD and TXD communication with the transmission module. The PB10 pin is used as the enable pin for the transmission chip.

The circuit configuration corresponding to the transmission module is shown in Fig. 5. MAX485CSA is used as the

communication chip, powered by 5V voltage, and filtered by a 0.1uf grounded capacitor in parallel. Pins 6 and 7 are used to receive data from STM32, and pins 2 and 3 are used to control data upload.

The circuit configuration corresponding to the power supply module is shown in Fig. 6. Dual batteries are adopted to provide power to the transmission module. With the input voltage ranging from 7V to 35V, a Lm7805 regulator is used to output 5V voltage for B1. Through AMS1117-3V3 with filter capacitors, 3.3V voltage is outputted, providing power to the sensor module and processing module. When there is a problem with power supply B1, battery B2 which can serve as a backup battery is switched on to maintain normal operation of all the other modules excluding the transmission module for a short period of time. Additionally, an LED light is used as a power indicator.

As to the PC module which is considered to be an upper computer, a portable computer equipped with an inter i5-11320H CPU and operating system window11 is used.

In terms of measuring the water content in crude oil, the traditional distillation method typically requires 3 hours, the Karl Fischer method generally takes 1 hour, while this device can obtain highly accurate results in just a few seconds.

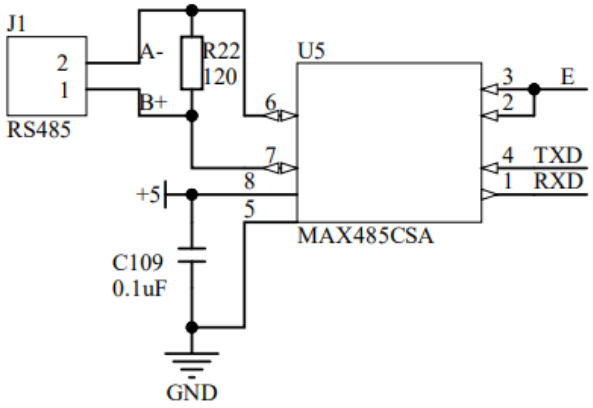

Fig. 5. MAX485 CSA circuit diagram.

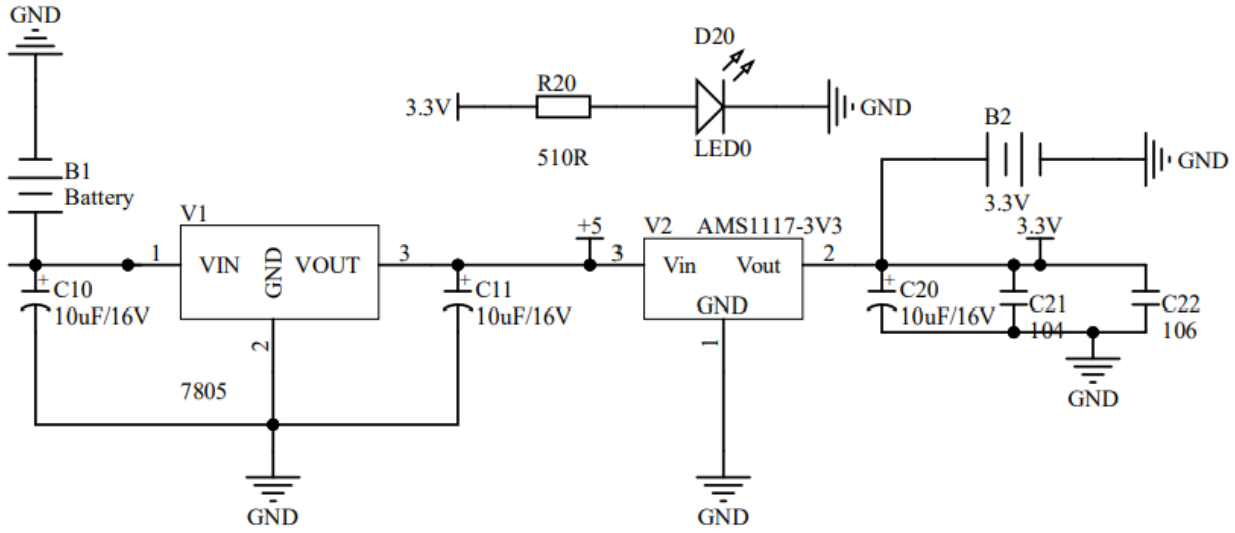

Fig. 6. Power supply circuit diagram.

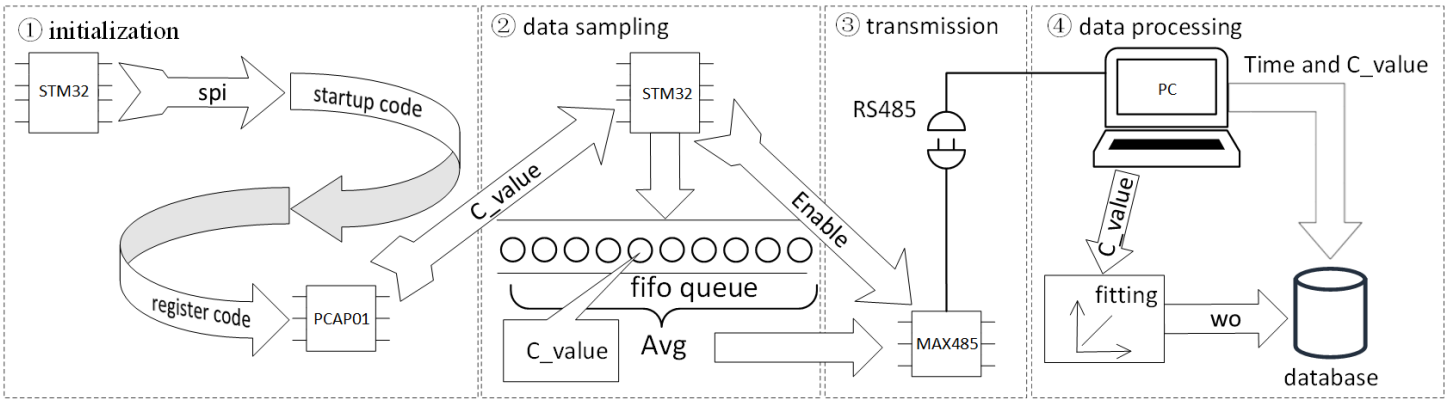

Fig. 7. System software diagram.

D. System Software Design

The software system is designed, as illustrated in Fig. 7. The entire process is primarily divided into four parts: (1) system initialization, (2) data sampling, (3) data transmission, and (4) data processing. The following content provides a detailed description of the four parts.

1) System initialization. Upon power-up, the system begins the initialization process. Initially, the STM32 chip attempts to establish SPI communication with the PCAP01 chip. The method involves sending a byte through SPI to a specific address on the PCAP01 chip, and then reading from that address. If the bytes sent and read match, the communication is deemed successful. Otherwise, if the communication fails, corresponding LED lights on the development board will indicate the SPI communication failure. Once the STM32 successfully establishes communication with the PCAP01, it will transmit the official 960-byte boot code to the PCAP01, followed by 11 pre-configured register codes. It is important to note that the 11 registers will utilize addresses ranging from zero to nine (also including 20).

2) Data sampling. Once the system initialization is complete, the sensor module where PCAP01 is located begins to capture capacitance values from the sensing probe every 400ns, transmitting the capacitance values which are expressed as "*C_value*" to the STM32 via SPI communication. Then, the STM32 sends the received capacitance values into a FIFO queue with a length of 10. When the queue is full, the values in the queue are averaged to reduce errors, then the arithmetic mean is transmitted to the MAX485. Meanwhile, an enable signal is provided to the MAX485.

3) Data transmission. Upon receiving data and enabling signal, MAX485 transmits data to PC through RS485.

4) Data processing. Upon receiving the capacitance data, the upper computer temporarily stores the reception time, inputs the data into the time-domain frequency fitting curve, and fits out the moisture content represented by the capacitance. The fitting principle will be detailed in the following part. Subsequently, the reception time, the capacitance data, and the calculated moisture content which is expressed as "wo" are jointly stored in the database for future reference.

E. Modeling Principle

The traditional univariate linear regression model is,

$$\hat{y} = b_1 x + b_0, \tag{4}$$

where $\hat{y}$ represents the dependent variable. x denotes the independent variable. b_1 and b_0 are the regression coefficient and the constant term, respectively. The error squared function Q of Eq. (4) satisfies,

$$Q = \sum (y_i - \hat{y}_i)^2, \tag{5}$$

b_1 and b_0 can be obtained by solving the system of equations,

$$\begin{cases} \dfrac{\partial Q}{\partial b_0} = 0 \\ \dfrac{\partial Q}{\partial b_1} = 0 \end{cases}, \tag{6}$$

and they can be substituted into Eq. (4) to get the estimated values of samples.

In order to enhance fitting accuracy, time-frequency domain analysis is employed for fitting. The principle of time-frequency domain analysis is elaborated below. The Taylor expansion of a univariate function is expressed as follows. If the function $u = f(x)$ has n+1 order derivatives in an open interval (a, b) containing x_0, then for any $x \in (a, b)$, it holds that,

$$f(x) = \frac{f(x_0)}{0!} + \frac{f'(x_0)}{1!}(x - x_0) + \frac{f''(x_0)}{2!}(x - x_0)^2 + \frac{f^{(n)}(x_0)}{n!}(x - x_0)^n + R_n, \tag{7}$$

where the remaining term R_n is expressed as

$$R_n = \frac{f^{(n+1)}(\delta)}{(n+1)!}(x - x_0)^{n+1}, \tag{8}$$

with δ between x and x_0. Correspondingly, the measured capacitance value and the water content of crude oil are expressed as c and α, respectively. For the hypothetical function of water content $\cdot\ \alpha = f(c)$, the Talor expansion can be carried out, and the second and higher expansion terms are ignored. That is

$$\alpha(c) = \frac{f(c)}{0!} + \frac{f'(c)}{1!}(x - c). \tag{9}$$

Therefore, Eq. (9) refers to the Taylor estimation expansion of the moisture content function.

As to the Fourier expansion of a unary function, a one-dimensional function on a finite interval satisfying Dirichlet conditions can be expanded as a linear combination of trigonometric functions. Therefore, the Fourier series corresponding to the one-dimensional function $u = f(x)$ defined on the interval $x \in [0, a)$ is,

$$f(x) = \sum_{n=-\infty}^{\infty} C_n e^{inx}, \tag{10}$$

where$n \in \alpha$, and $C_n = \frac{1}{2\pi}\int_{-\pi}^{\pi} f(x)e^{-inx}dx$.

Correspondingly, the water content is assumed to be a Fourier series expansion, when ignoring the expansion terms with |n| > 2. That is

$$\alpha(c) = \frac{1}{2\pi}\int_{-\pi}^{\pi} f(x)dx + \frac{1}{2\pi}\int_{-\pi}^{\pi} f(x)e^{-ix}dx * e^{ic}, \tag{11}$$

where c and α represent the measured capacitance value and the water content in crude oil, respectively. Eq. (11) is the Fourier estimation expansion of the moisture content function.

Taylor expansion is a signal expansion method in the time domain; while, Fourier expansion is a signal expansion method in the frequency domain. The two expansion methods can be combined through the idea of one-dimensional nonlinear regression. Let

$$r_1 = c, r_2 = e^{ic}. \tag{12}$$

By making the arithmetic average of Eq. (9) and Eq. (11), the water content in crude oil can be expressed as

$$\alpha(r_1, r_2) = k_0 + \sum_{i=1}^{2} r_i k_i\,, \tag{13}$$

where k_1 and k_2 are the coefficients of the corresponding terms in Eq. (9) and Eq. (11), respectively. k_0 is the constant term. Since the objective function in actual calculations is a real-valued function, the imaginary coefficients in the frequency domain expansion terms can be set to 0. Calculations are only performed on the real parts. That is

$$Lm[e^{ic}] = \cos(c) + isin(c) = cosc, \tag{14}$$

where $Lm[\cdot]$ means taking the real part.

Eq. (13) conforms to the form of the univariate linear regression model in Eq. (4). Correspondingly, the squared error function Q satisfies

$$Q = \sum(\alpha - \bar{\alpha})^2\,. \tag{15}$$

The estimated value $\overline{k_0}$, $\overline{k_1}$ and $\overline{k_2}$ are obtained by solving the equation system

$$\begin{cases} \dfrac{\partial Q}{\overline{k_0}} = 0 \\ \dfrac{\partial Q}{\overline{k_1}} = 0\,. \\ \dfrac{\partial Q}{\overline{k_2}} = 0 \end{cases} \tag{16}$$

Correspondingly, the estimation function for measuring water content in crude oil can be obtained.

III. Experimental Results

In order to verify the effectiveness of our method in measuring the moisture content of aqueous crude oil, a device for measuring the moisture content of aqueous crude oil has been designed based on STM32 and PCAP01. In the experiment, PCAP01 is set to a drift mode, and the reference capacitance is 47Pf. In order to avoid the influence of ambient temperature, all the following experimental measurement steps are carried out in a constant temperature environment. The specific experimental process is as follows. Firstly, use dehydrated crude oil and pure water to configurate the crude oil mixture with different water content. Secondly, pour the configured crude oil mixture with different moisture content into the prepared cylindrical glass container. Thirdly, fit the capacitor probe tightly to the glass container to avoid the interference of air on the measurement results. Fourthly, start the device for measuring and record the measurement results. After the measurement, the glass container is replaced to measure the moisture content of other crude oil mixtures. In the actual measurement, the capacitance value takes on decimal place. The measurement results are shown in Table I.

From Table I, it can be seen that when the crude oil mixture oil is a continuous phase, the measurement results of different water contents have a large gap. This is because the dielectric constant of crude oil is much smaller than the dielectric constant of water at room temperature. When the water content rises, a small amount of water causes a large change in the relative dielectric constant of the mixed liquid, resulting in a more drastic change in capacitance.

TABLE I. One-Time Restes Result

water/ml	oil/ml	moisture content	capacitance/pf
0	575	0	28.9
125	450	0.217391	30.8
225	350	0.391304	37.2
275	300	0.478261	40.7
325	250	0.565217	43.4
375	200	0.652174	46.6
425	150	0.73913	47.2
475	100	0.826087	50.2
525	50	0.913043	53.8
555	20	0.965217	54.9
565	10	0.982609	56.3
575	0	1	57.3

Correspondingly, the data in Table I is fitted by univariate linear fitting (ULF). The fitting result is illustrated in Fig. 8.

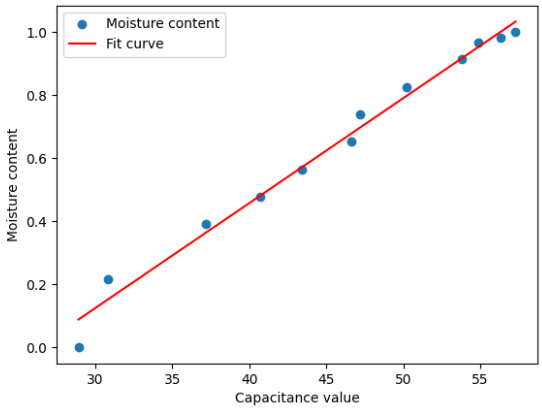

Fig. 8. The result using univariate linear fitting.

The data in Table I is fitted in the time domain (TD) with logarithmic $\alpha = lnc$, and the fitting formula is given by Eq. (9). The fitting result is shown in Fig. 9.

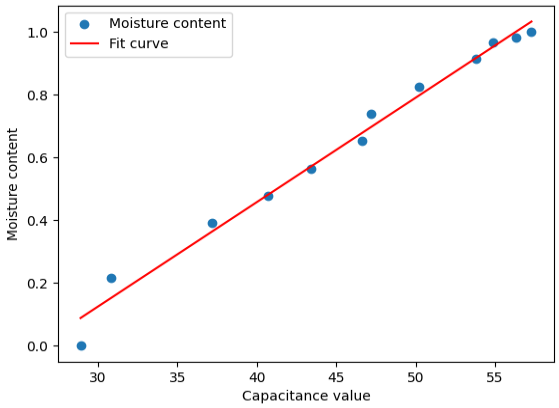

Fig. 9. The result fitted in the time domain.

In addition, the data in Table I is fitted in the frequency domain (FD) with logarithm $\alpha = lnc$, and the fitting formula corresponds to Eq. (11) and Eq. (14). Because the capacitance value cannot be measured negative, so$c \in [0, 60$. The fitting result is illustrated in Fig. 10.

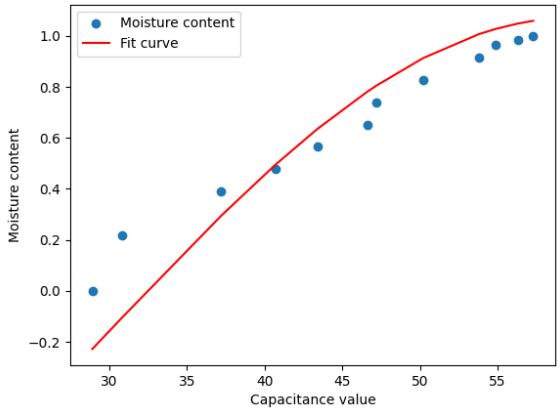

Fig. 10. The result fitted in the frequency domain.

Besides, the data in Table I is fitted in the time-frequency domain (TFD), and the fitting formula is given by Eq. (13). The fitting result is shown in Fig. 11. For further comparison, a logarithmic linear fitting (LLF) is also made. The fitting result is illustrated in Fig. 12. All the obtained fitting results and the quantitative results are listed in Table II. It can be seen that the model fitted in TFD gets the best result.

Table III illustrates the experimental results of ten sets of crude oil samples from ten different mines.

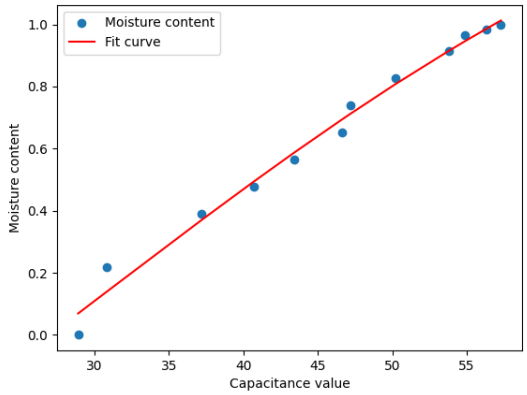

Fig. 11. The resultfitted in the time-frequency domain.

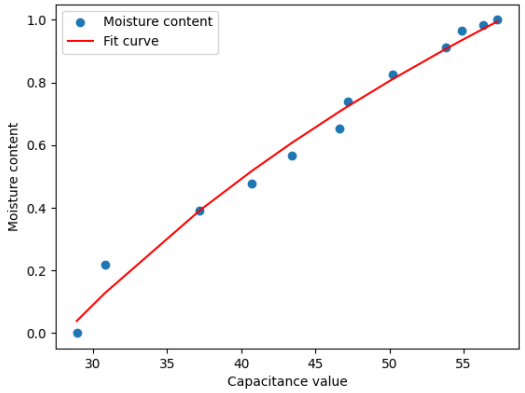

Fig. 12. The comparing result fitted in a logarithmic linear fitting.

TABLE II. FITTING AND QUANTITATIVE RESULTS

Fitting mode	Fitting formula	r^2
ULF	$\alpha = 0.033c - 0.8724$	0.9847
TD	$\alpha = 0.0325(c - 0.01214) + 3.1651$	0.9847
FD	$\alpha = 2 * (ln2 - 1) * cos\frac{\pi c}{60} + 2 * (ln2 - 1) * sin\frac{\pi c}{60} - 0.156$	0.8099
TFD	$\alpha = 0.249 * cos\frac{\pi * c}{60} + 0.399985 * sin\frac{\pi * c}{60} + 0.05512 * (x - 107.09) - 3.955$	0.9871
LLF	α=1.3974lnc-4.6619	0.9850

TABLE III. EXPERIMENTAL RESULTS

Fitting mode	ULF	TD	FD	TFD	LLF
r^2	0.9864	0.9864	0.8146	0.9882	0.9864
	0.9831	0.9831	0.8096	0.9857	0.9847
	0.9729	0.9729	0.8265	0.9785	0.9778
	0.9871	0.9871	0.8190	0.9892	0.9865
	0.9827	0.9827	0.8049	0.9860	0.9845
	0.9835	0.9835	0.8064	0.9856	0.9834
	0.9838	0.9838	0.8062	0.9862	0.9839
	0.9859	0.9859	0.8074	0.9880	0.9853
	0.9813	0.9813	0.8148	0.9824	0.9793
	0.9836	0.9836	0.8132	0.9863	0.9849

As can be seen from Table III, the crude oil mixture with the same water content has a certain impact on the capacitance measurement results due to the different mineralization degree and salt content of the crude oil collected at different times. Besides, the method corresponding to the time-frequency domain analysis still has more advantages in fitting accuracy with higher accuracy and better fitting effect than monadic linear regression, time-domain regression, frequency-domain regression and logarithmic linear regression, which demonstrates the effectiveness of our method.

IV. CONCLUSION

In this paper, a crude oil water content measuring equipment is designed based on STM32 and PCAP01. Besides, a time-frequency domain regression model for data processing is presented. Together with the established system software, they form a capacitance-based system for measuring crude oil moisture. As the sensor core, PCAP01 which has strong anti-interference ability is used. PCAP01 chip adopts shock discharge method to measure capacitance, which can effectively prevent impurities from being adsorbed near the electrode plate. In addition, a slotted cylindrical electrode plate is used in the sensor probe. The electrode plate is tightly fitted to the cylindrical glass wall, which eliminates the interference caused by air. The sensor adopts non-contact method to measure capacitance, which avoids the problem of electrode plate cleaning. After the device collects the capacitance data, STM32 preprocesses the data, and then inputs the preprocessed capacitance values into the proposed time-frequency domain regression model. Experimental results show that the fitting accuracy and reliability of the time-frequency domain regression model are better than that of the monadic linear regression model, the time-frequency domain regression model, the frequency-domain regression model and the logarithmic regression model in the moisture content range between 0 and 100%. Especially for samples of crude oil with fewer impurities, the fitting accuracy and reliability of the time-frequency domain regression model reach their optimal levels.

In the follow-up experiments, we will add a variety of sensors to measure factors such as temperature and flow rate, explore the influence of these factors on capacitance measurement through experiments, and seek the functional relationship between the influencing factors and capacitance measurement, so as to further improve the measurement accuracy and anti-interference ability of the device.

REFERENCES

[1] Q. S. Zhu, W. X. Wang, X. J. Yin, and Z. X. Yang, "Review and prospect of determination methods of water content in crude oil," in *2021 2nd International* Conference on Artificial Intelligence and Computer Engineering (ICAICE), Nov. 2021, pp. 227–230.

[2] K. Li and Y. Li, "Effect of initial water saturation on crude oil recovery and water cut in water-wet reservoirs," International Journal of Energy Research, vol. 38, no. 12, pp. 1599–1607, Oct. 2014.

[3] B. Kamal, Z. Abbasi, and H. Hassanzadeh, "Water-Cut Measurement Techniques in Oil Production and Processing-A Review," Energies, vol. 16, no. 17, p. 6410, Sep. 2023.

[4] Z. L. Zhen, H. F. Wang, Y. M. Yue, D. M. Li, X. P Song, and J. Li, "Determination of water content of crude oil by azeotropic distillation Karl Fischer coulometric titration," Analytical and Bioanalytical Chemistry, vol. 412, no. 19, pp. 4639–4645, Jul. 2020.

[5] Y. Luo, L. Wang, H. Wang, and X. Yuan, "Simultaneous optimization of heat-integrated crude oil distillation systems," Chiese Journal of Chemical Engneering, vol. 23, no. 9, pp. 1518–1522, Sep. 2015.

[6] Y. Wang, C. Li, and B. R Zhao, "Measurement of water content of crude oil using quartz crystal microbalance," Sensors and Materials, vol. 34, no. 3, pp. 1033-1042, Mar. 2022.

[7] Z. Q. Lu *et al.*, "Non-contact measurement of the water content in crude oil with all-optical detection," Energy Fuels, vol. 29, no. 5, pp. 2919–2922, May 2015.

[8] C. A. B. Reyna, E. E. Franco, A. L. Duran, L. O. V. Pereira, M. S. G. Tsuzuki, and F. Buiochi, "Water content monitoring in water-in-Oil emulsions using a piezoceramic sensor," Machines, vol. 9, no. 12, pp. 335 Dec. 2021.

[9] C. A. B. Reyna, E. E. Franco, M. S. G. Tsuzuki, and F. Buiochi, "Water content monitoring in water-in-oil emulsions using a delay line cell," Ultrasonics, vol. 134, pp. 107081, Sep. 2023.

[10] Yu. V. Makeev, A. P. Lifanov, and A. S. Sovlukov, "Microwave measurement of water content in flowing crude oil," Autom Remote Control, vol. 74, no. 1, pp. 157–169, Jan. 2013.

[11] R. K. Abdulsattar, T. A. Elwi, and Z. A. Abdul Hassain, "A new microwave sensor based on the moore fractal structure to detect water content in crude oil," Sensors, vol. 21, no. 21, pp 7143, Jan. 2021.

[12] J. Austin, S. Rodriguez, P.-F. Sung, and M. Harris, "Utilizing microwaves for the determination of moisture content independent of density," Powder Technology, vol. 236, pp. 17–23, Feb. 2013.

[13] Y. Zhang and S. Okamura, "A Density-Independent Method for High Moisture Content Measurement Using a Microstrip Transmission Line," Journal of Microwave Power and Electromagnetic Energy, vol. 40, no. 2, pp. 110–118, 2006.

[14] Q. Zeng, G. Li, Q. Liu, H. Jiang, and Z. Wang, "Measurement system of ultra-low moisture content in oil based on the microwave transmission method," Microwave and Optical Technology Letters, vol. 65, no. 1, pp. 47–53, 2023.

[15] D. Sudac *et al.*, "On-line determination of the water cut and chlorine impurities in crude oil using a pulsed beam of fast neutrons," Applied Radiation and Isotopes, vol. 200, pp. 110965, Oct. 2023.

[16] J. Han, Y. Z. Li, Z. M. Cao, Q. Liu, H. W. Mou, "Water content prediction for high water-cut crude oil based on SPA-PLS using near infrared spectroscopy," Spectroscopy and Spectral Analysis, vol. 39, no. 11, pp. 3452-3458, 2019.

[17] W. J. Jin, K. Zhao, C. Yang, C. H. Xun, H. Ni, and S. H. Chen, "Experimental measurements of water content in crude oil emulsions by terahertz time-domain spectroscopy," Applied Geophysics, vol. 10, no. 4, pp. 506–509, Dec. 2013.

[18] L. Guan, H. Zhan, X. Miao, J. Zhu, and K. Zhao, "Terahertz-dependent evaluation of water content in high-water-cut crude oil using additive-manufactured samplers," Science China-Physics Mechanics&Astronomy, vol. 60, no. 4, p. 044211, Apr. 2017.

[19] F. Sun and S. Tang, "Design of crude oil water content measuring chip based on RF method," Measurement Science and Technology, vol. 35, no. 1, pp. 015907, Oct. 2023.

[20] N. Azmi, L. M. Kamarudin*et al.*, "RF-Based Moisture Content Determination in Rice Using Machine Learning Techniques-Web of Science Core Collection," Sensors, vol. 21, no. 5, pp. 1875, Apr. 2021.

[21] C. V. K. Kandala and S. O. Nelson, "RF impedance method for estimating moisture content in small samples of in-shell peanuts," IEEE Transactions on Instrumentation and Measurement, vol. 56, no. 3, pp. 938–943, Jun. 2007.

[22] Q. Liu, B. Chu, J. Peng, and S. Tang, "A visual measurement of water content of crude oil based on image grayscale accumulated value difference," Sensors, vol. 19, no. 13, pp. 2963, Jan. 2019.

[23] M. Z. Aslam and T. B. Tang, "A high resolution capacitive sensing system for the measurement of water content in crude oil," Sensors, vol. 14, no. 7, pp. 11351-11361, Jul. 2014.

[24] A. Semenov, O. Zviahin, N. Kryvinska, O. Semenova, and A. Rudyk, "Device for measurement and control of humidity in crude oil and petroleum products," Metrology and Measurement Systems, pp. 195–208, Feb. 2023.

[25] C. Lesaint, W. R. Glomm, L. E. Lundgaard, and J. Sjoblom, "Dehydration efficiency of AC electrical fields on water-in-model-oil emulsions," Colloids and Surfaces A-Physicochemical and Engineering Aspects, vol. 352, no. 1–3, pp. 63–69, Dec. 2009.

[26] C. Lesaint, G. Berg, L. Lundgaard, and M.-H. G. Ese, "A Novel Bench Size Model Coalescer: Dehydration Efficiency of AC Fields on Water-in-Crude-Oil Emulsions," IEEE Transactions on Dielectrics and Electrical Insulation, vol. 23, no. 4, pp. 2015–2020, Aug. 2016.

[27] C. T. Chiang and Y. C. Huang, "A semicylindrical capacitive sensor with interface circuit used for flow rate measurement," IEEE Sensors Journal, vol. 6, no. 6, pp. 1564–1570, Dec. 2006.